# Photophysics of Phenylpyrrole Derivatives and Their Acetonitrile Clusters in the Gas Phase and in Argon Matrixes: Simulations of Structure and Reactivity

### D. Schweke and Y. Haas*

*Department of Physical Chemistry and the Farkas Center for Light Induced Processes,*
*The Hebrew University of Jerusalem, Jerusalem, Israel 91904*

### Bernhard Dick

*Lehrstuhl für Physikalische Chemie, Universität Regensburg, Regensburg, Germany 93040*

Recent experiments on the dual fluorescence of phenylpyrrole (PP) and pyrrolobenzonitrile (PBN) in supersonic jets and in cryogenic matrixes are analyzed. The structures of the 1:1 clusters are calculated using ab initio, density functional theory (DFT) and molecular mechanics (MM) methods. In these calculations, the structures of PP and PBN in the ground state and in two possible minima on the charge-transfer excited state are taken from a recent theoretical analysis. The structures of PP and PBN clusters with a larger number of acetonitrile molecules are also calculated using the molecular mechanics method. It is shown that the fact that small PP:AN and PBN:AN clusters do not exhibit any charge-transfer (CT) type emission, whereas for PBN:AN$_n$ clusters (n ≥ 4) CT emission is observed, can be understood on the basis of the calculated structures. The trapping of PP and of PBN in an argon matrix (neat and doped with acetonitrile) is simulated by a molecular dynamics procedure. The observation of locally excited (LE) fluorescence only from PP in neat argon, whereas from argon-trapped PBN *both* CT and LE emission bands are observed, is readily understood on the basis of these simulations. Moreover, the appearance of CT emission from PP-doped argon matrixes when acetonitrile is added is also explained, as well as the relatively small spectral shift observed upon addition of acetonitrile to PBN-doped argon matrixes.

## I. Introduction

Photoinduced intramolecular charge transfer (ICT) is accompanied by electronic and structural changes in the molecule.[1,2] This process is therefore strongly affected by interactions with the surrounding, for instance by the polarity of the solvent. Derivatives of benzene wherein an electron-donating group and an electron-accepting group are substituted para to each other are among the most extensively studied series of molecules for which this phenomenon was observed.[1] *N*-Phenylpyrrol (PP) and its derivative 4-(1*H*-pyrrol-1-yl)benzonitrile (abbreviated PBN) belong to this class of molecules. Both molecules have been studied in the gas phase, isolated in a supersonic jet,[3] in clusters with acetonitrile,[4] (AN) and in solution[5−8] (polar and nonpolar solvents). These molecules are also the first of their class to have been studied in cryogenic matrixes (both neat argon and argon doped by AN).[9,10]

Both molecules show only LE-type fluorescence when isolated from any interaction with the surrounding in a supersonic jet,[3,11] indicating that the CT state is higher than the LE one in the bare molecules. In contrast, the emission observed from clusters with AN (created by co-expanding the PP or PBN molecule with AN) is drastically different for the two molecules: whereas PP:AN$_n$ clusters and PBN:AN$_n$ ($n ≤ 4$) exhibit only single band emission, two separate bands were observed from PBN:AN$_n$ clusters for $n > 4$.[4] This different conduct was assigned to the stronger accepting power of the benzonitrile moiety compared to the phenyl one.

The difference between the two molecules was also noted in the solution phase: in nonpolar solvents such as cyclohexane,

the PP emission spectrum is largely due to the locally excited (LE) state, whereas the PBN one is mostly due to the charge-transfer (CT) state.[8] In polar solvents such as acetonitrile, the CT emission band is broad and strongly red-shifted for PBN, whereas it appears only as a small shoulder in the red edge of the emission spectrum of PP. In an argon matrix, the spectrum of PP is very similar to the one recorded in the jet (except for a matrix shift), indicating that emission is from the LE state, whereas the spectrum of PBN is dominated by a broad, almost structureless strong band, attributed to the CT state, which is accompanied by a much weaker LE one.[9,10] Addition of AN to the argon matrix did not result in a significant change in the emission spectrum of PBN, whereas it led to a dramatic change in the spectrum of PP: A new broad band appeared, assigned to the CT state, and the intensity ratio of the LE to CT bands was strongly excitation wavelength dependent.

The new set of experimental data obtained at low temperatures (∼20 K), calls for a model that can account for all the data. In an attempt to do so on the molecular level, this paper reports the calculations of the optimized cluster structures of both PP and PBN with *n* AN molecules for $n = 1−6$. This structural investigation was combined with MD simulations of the trapping sites of PP, PBN, and their 1:1 clusters with AN in an argon matrix.

Theoretical interpretations for the dual fluorescence phenomenon in PP, PBN, and related molecules have been discussed extensively.[1] It is accepted that one emission band is due to a LE state derived from the $1^1B_{2u}$ excited state of benzene. This state is often referred to as the B state. The "anomalous", red-

Photophysics of Phenylpyrrole Derivatives

*J. Phys. Chem. A, Vol. 109, No. 17, 2005* **3831**

shifted emission is due to a CT state derived from the $1^1B_{1u}$ state of benzene and is usually referred to as the A state. One of the controversial issues is the nature of the CT state. Two leading models for the CT state have been advanced: one contends that the benzene and pyrrolo rings are perpendicular to each other (twisted intramolecular charge transfer, TICT[12]); the other, that the CT state is planar (planar intramolecular charge transfer, PICT[2]). In the Zilberg−Haas[13] model, both options were shown to be possible on the A-state potential surface that was calculated to have two minima, one planar and the other with a perpendicular (twisted) structure. The planar minimum has a quinoidal structure, i.e., shortened central bonds of the benzene ring and a short C−$N_{pyrrol}$ bond, and is termed the Q form. The twisted one has an antiquinoid structure with lengthened central benzene bonds and C−$N_{pyrrol}$ bond and is labeled as the AQ form. Both minima are on the same potential surface, the first electronically excited A state. In the isolated molecule, the planar structure (Q form) is lower in energy but has a smaller dipole moment.

In this paper experimental results in the jet and in the matrix are analyzed in view of the theoretical calculations. Some of the pertinent issues which are addressed in this article are the following:

(1) Why is the emission observed from PBN:$AN_n$ ($n > 4$) clusters composed of two separate bands, assigned to the LE and CT states, whereas emission from clusters of PP with AN of any size consists of a single band (assigned to the LE band[4])?

(2) Why is the excitation spectrum of the clusters ($n = 1−5$) completely devoid of vibrational structure?

(3) Why is CT emission observed from PBN in a neat argon matrix and not from PP?

(4) Why does addition of AN to the argon matrix result in a very different emission spectrum (and strongly dependent on the excitation wavelength) in the case of PP, whereas the emission spectrum of PBN changes only slightly?

(5) What is the nature of the CT state in argon (quinoid-planar or antiquinoid-perpendicular)?

(6) What are the implications of the molecular-scale study on the experimental results in solution?

The structure of the paper is as follows: In section II details of the computational methods are given. Section III summarizes the numerical results obtained for clusters of PP and PBN with AN, in the ground state and in the CT states. The structure and dipole moment of the LE state are similar to those of the ground state, so that its clusters with acetonitrile were not calculated separately. These results are used to calculate the trapping sites of PP, PBN, and their 1:1 AN clusters in an argon matrix. Section IV discusses the implications of these results on the photophysical properties of PP and PBN in clusters and matrixes and compares them with experimental data. A brief discussion of consequences of these data to liquid solutions is also included. Section V gives an overall summary of the results.

## II. Computational Details

**(A) Optimization Method.** Quantum chemical (QC) computations were performed, using the Gaussian 98 program suite,[14] for the electronic ground-state (GS) structures of PP and PBN as well as for the 1:1 clusters with AN. The equilibrium geometries were calculated by the density functional theory[15,16] (DFT) using the B3LYP hybrid functional and by the Hartree−Fock method expanded by second-order Møller−Plesset perturbation theory (HF-MP2).[17] For the DFT calculation the basis sets used were correlation-consistent double-$\zeta$ (cc-pVDZ) and Dunning's augmented with diffuse functions (aug-cc-pVDZ),

**TABLE 1: List of the Atomic Parameters Used in Equation 1 for AN, PP, and PBN Molecules**

| molecule | site | $\sigma$ (Å) | $\epsilon$ (kcal/mol) |
|---|---|---|---|
| acetonitrile[19] | $C_{CH_3}$ | 3 | 0.1 |
| | $C_{CN}$ | 3.4 | 0.1 |
| | N | 3.3 | 0.1 |
| | H | 2.2 | 0.02 |
| prrrole[17] | C | 3.55 | 0.07 |
| | N | 3.25 | 0.17 |
| | H | 2.42 | 0.03 |
| benzene[18] | C | 3.55 | 0.07 |
| | H | 2.42 | 0.03 |
| benzonitrile[18] | C | 3.55 | 0.07 |
| | $C_{CN}$ | 3.65 | 0.15 |
| | N | 3.25 | 0.17 |
| | H | 2.42 | 0.03 |

whereas only the former was applied for the HF-MP2 calculation (due to CPU and memory limitation). The energy was always computed after the geometry was optimized at the corresponding level of theory to prevent energy variations due to small structural changes. For the DFT computation of the 1:1 cluster structures several arbitrary arrangements of AN relative to the pyrrole derivative were taken as initial guesses of the cluster's structure. The harmonic frequencies of each optimized structure were calculated by using the analytic second-derivative matrix along the nuclear coordinates. If the optimized structure had one or more imaginary frequencies, the structure was further optimized until the true local minimum was obtained (all the vibrational frequencies were found to be real). The binding energies (BE) of the clusters were obtained by subtracting the energies of the monomers from those of the complexes and correcting for the basis set superposition errors (BSSE) using the counterpoise scheme of Boys and Bernardi.[18]

Molecular mechanics (MM) computations were also performed for optimizing the structures of the PP:$AN_n$ and PBN:$AN_n$ clusters for $1 \leq n \leq 6$. For these calculations, the following intermolecular potential was used:

$$V_{int} = \sum_{a \in A}\sum_{b \in B}\left\{\frac{1}{4\pi\epsilon_0}\frac{q_a q_b e^2}{R_{ab}} + 4\epsilon_{ab}\left[\left(\frac{\sigma_{ab}}{R_{ab}}\right)^{12} - \left(\frac{\sigma_{ab}}{R_{ab}}\right)^6\right]\right\} \quad (1)$$

where $R_{ab}$ is the distance between atoms a and b, belonging to molecules A and B, respectively, $\epsilon_{ab}$ is the well depth of the Lennard-Jones (LJ) interaction potential between the two atoms, $\sigma_{ab}$ is the distance at which the LJ potential equals zero, and $q_i$ is the electronic charge on atom i. During cluster optimization, the molecules PP, PBN, and AN were considered rigid. Therefore, the interaction potential between atoms on the same molecule was not included in eq 1.

$\epsilon_{ab}$ and $\sigma_{ab}$ are given by the usual combination rules: $\epsilon_{ab} = \sqrt{\epsilon_{aa}\epsilon_{bb}}$ and $\sigma_{ab} = (1/2)(\sigma_{aa} + \sigma_{bb})$. The potential parameters, $\epsilon$ and $\sigma$, were taken from OPLS (optimum parameters for liquid simulations) of pyrrole,[19] benzene,[20] and benzonitrile,[20] whereas Bohm parameters[21] were used for AN. The corresponding values are presented in Table 1. The initial geometries for the ground-state PP and PBN molecules were obtained from the DFT calculations. ESP (electrostatic potential) atomic charges, computed by Kollman and Singh's[22] method (see Figure S1 of the Supporting Information), were used in the calculation. The position of each AN ligand was described (in the reference frame defined by the heavy molecule) by one distance vector and one set of Euler angles (rigid body approximation). In general, 200 initial geometries (randomly generated) were optimized to find the most stable one. The optimization was performed using two

different algorithms developed by Powell[23,24] and implemented by available codes.[25] The same method was used to evaluate the geometry of clusters of PP or PBN excited to the CT state with AN. Two CT state structures were used: a perpendicular (antiquinoid, AQ) one and a planar (quinioid, Q) one, both shown to be possible on the A-state potential surface by a recent QC analysis.[13] The geometries of both forms were calculated at the CASSCF (12,12) level and the ESP charges computed for each electronic state. The potential parameters were the same as in the ground state. This approximation is expected to retain the main differences between the two molecules, even if the results for both in the excited state may be numerically inaccurate. The binding energies were in all cases calculated by the difference between the energy of the minimum and the sum of the separate constituents.

**(B) MD Simulation of Matrix Sites.** The computational procedure for simulation of the matrix sites was described previously in detail.[26,27] To reproduce the experimental distribution of sites (which is controlled kinetically), the deposition temperature was 5 K and the fast cooling method[26] was applied. In the simulation process it is convenient to use the {001} plane as the exposed surface but experimental evidence indicates that the {111} plane is the exposed one during a gas-phase deposition of argon.[28] To minimize a possible bias due to the choice of the {001} plane as the exposed surface, the simulation was begun by randomly depositing 50 argon atoms prior to bringing in the guest molecule. All molecules or clusters were treated as rigid bodies (the constraints were imposed by the RATTLE algorithm[29]). The cluster structures used were those having the most stable forms as obtained by the MM optimization described above. The procedure for calculating the relative stabilization of the trapping sites was described in detail in refs 26 and 27.

## III. Results

In this section the results of the computations are presented. Clusters of the pyrrole derivatives with $n$ AN molecules will be denoted by PP:AN$_n$ or PBN:AN$_n$. In cases where several structural isomers are possible, the most stable one will be referred to as I, a higher lying one as II, etc. For instance, the most stable cluster of PP with 3 AN ligands will be denoted as the PP:AN$_3$(I) cluster. When many clusters of similar binding energies are found a histogram showing the frequency at which different clusters were encountered in the simulation is presented, and representative structures are picked for the discussion.

Matrix trapping sites will be classified according to their size (given by the number of argon atoms removed to allow space for the inserted molecule) and their relative energies. Sites of a given size are distinguished by their energy ordering designated alphabetically: the lowest energy site (largest stabilization) is denoted by a, the next by b, etc. Thus the most stable six-substitutional site is the 6a trapping site, and the one whose energy stabilization is second is denoted as 6b, etc.

**(A) Cluster Structures.** Cluster structures were calculated both for the electronic ground state (GS) of the pyrrole derivatives and for the two CT states (Q and AQ). The ground-state clusters are denoted as explained above with the prefix GS added (e.g. GS P:AN$_n$(X)); The excited-state clusters are denoted by adding Q or AQ as prefix. In cases where no possible ambiguity may arise, the GS prefix is omitted from the description of ground-state clusters.

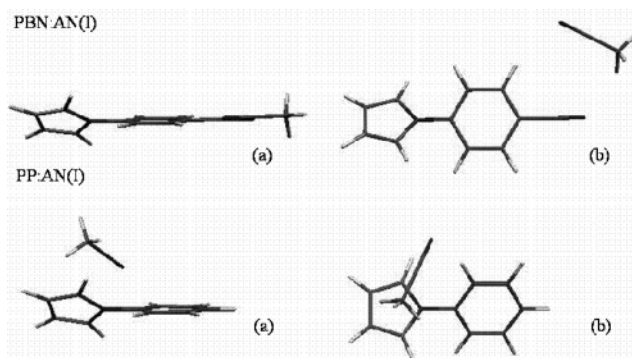*(1) Clusters of Ground-State PP or PBN with One AN Molecule.*



**Figure 1.** Structures of the most stable isomers of PBN:AN (top) and PP:AN (bottom) 1:1 clusters, according to the MM calculation. A side view (a) and a top view (b) of each cluster are shown.
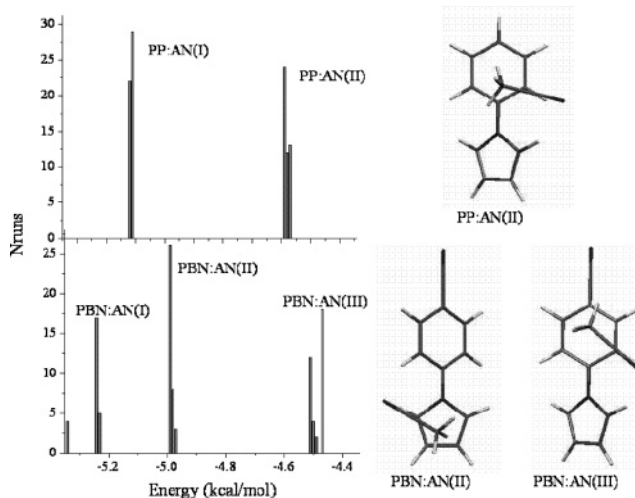


**Figure 2.** Left: Histograms of the PBN:AN and PP:AN 1:1 clusters calculated by the MM procedure (for 200 runs with different initial geometries). The histograms show the number of runs (Nrun) that led to a cluster of given energy. The width of each energy bin is 0.05 kcal/mol. Different isomers are indicated by different Roman numerals. Right: The structures of some high-energy isomers of PBN:AN and PP:AN.

*(1.1) Molecular Mechanics Optimization.* The most stable optimized structures of the PP:AN and PBN:AN 1:1 adducts obtained from the MM calculation are shown in Figure 1. In the PP:AN cluster, the acetonitrile molecule is located close to the pyrrole ring with the methyl group approximately above the ring center (C−H···$\pi$ interaction) and the cyano group pointing toward the closest hydrogen atoms from the two rings. The distance between the centers of mass of the PP and AN molecules is 3.92 Å. The structure of the PBN:AN cluster is very different: the AN molecular axis lies approximately in the plane of the benzene ring, and the molecule is located close to the cyano group; Its methyl group lies next to the cyano group of PBN, whereas its nitrile end is near the ortho hydrogen of the phenyl ring. The distance between the centers of mass of PBN and AN is 6.37 Å. The calculated cluster binding energies (BE) are −5.1 kcal/mol in the case of PP and −5.3 kcal/mol in the case of PBN values, which are slightly less than BE of the AN dimer (−5.6 kcal/mol [30]). Figure 2 shows the structures of some higher lying local cluster minima and a histogram of the optimization results. In the PP:AN(II) isomer the acetonitrile molecule is located above the benzene ring. This structure is similar to the benzene:AN cluster reported by El-Shall et al.[31] The PBN:AN(II) isomer resembles closely the most stable PP:AN(I) cluster with the AN close to the pyrrole ring. The binding energies are practically equal in those two structures: −5.0 and

Photophysics of Phenylpyrrole Derivatives

*J. Phys. Chem. A, Vol. 109, No. 17, 2005* **3833**

**TABLE 2: Binding Energies (kcal/mol), Including BSSE Correction, for the PP:AN and PBN:AN Ground-State Clusters**[a]

| | PP:AN | | PBN:AN | |
| --- | --- | --- | --- | --- |
| | total energy (hartrees) | binding energy (kcal/mol) | total energy (hartrees) | binding energy (kcal/mol) |
| level of theory | | | | |
| B3LYP/cc-pVDZ | -574.0142 | -3.26 | -666.2674 | -5.77 |
| B3LYP/aug-cc-pVDZ | -574.0453 | -2.76 | -666.3028 | -4.83 |
| MP2/cc-pVDZ | -572.2356 | -7.09 | -664.2443 | -7.27 |

[a] The energy was computed at each level of theory after full optimization of the geometry structure.
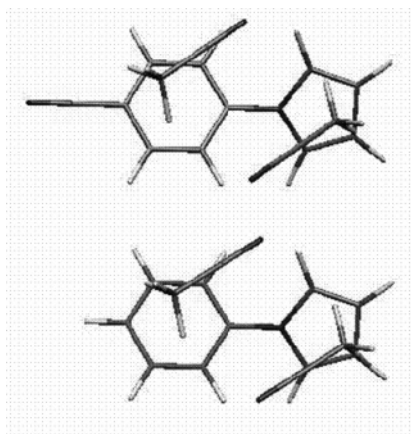


**Figure 3.** Calculated structures of the energetically most stable isomer of PBN:AN$_2$ (top) and PP:AN$_2$ (bottom) clusters.

-5.1 kcal/mol, respectively. Finally, in the PBN:AN(III) cluster, the AN is located near the benzene ring (as in PP:AN(II)).

(1.2) DFT and HF-MP2 Results. The most stable 1:1 cluster structures obtained from the QC computations were similar to those obtained from the MM calculation. A detailed comparison between the structures is deferred to the Discussion. Table 2 lists the binding energies (BE), including BSSE correction, obtained from the DFT/B3LYP and HF-MP2 methods. The calculated binding energy dependence on the size of the basis set is demonstrated in the results of the DFT calculation: Addition of diffuse functions results in the lowering of the binding energy. In both DFT and HF-MP2, the PBN:AN cluster is computed to have a larger binding energy than the PP:AN one, but the energy difference between those two clusters amounts to ~2 kcal/mol according to DFT, whereas it is only 0.2 kcal/mol with HF-MP2.

*(2) Clusters of Ground-State PP or PBN with Two AN Molecules (MM Method).* The structures of all clusters having more than one AN ligand were calculated using the MM method. The optimized geometries found for PP:AN$_2$(I) and PBN:AN$_2$-(I) were nearly identical (Figure 3). The two AN molecules are located on the same side of the pyrrole derivative, with the methyl groups above each of the aromatic rings. The total binding energy is -13.55 kcal/mol for PP:AN$_2$ and -14.00 kcal/mol for PBN:AN$_2$. In these clusters, the structure and binding energy (-5.5 kcal/mol) of the AN pair is very similar to those of the isolated AN dimer,[30] indicating that the presence of the benzopyrrole molecule hardly alters the AN dimer structure; a similar trend was observed for the most stable benzene:AN$_2$ cluster reported by El-Shall et al.[31] In addition to the most stable cluster, various additional structures were obtained for the PP:AN$_2$ and PBN:AN$_2$ isomers as shown in the histograms of Figure 4. In a range of up to 7% above the lowest energy minimum, the structures are very similar to that of the most
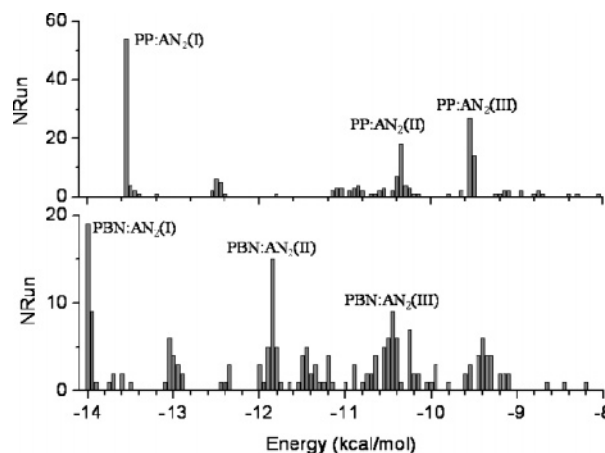


**Figure 4.** Histograms of the calculated isomers of PBN:AN$_2$ and PP:AN$_2$ obtained from 200 runs with different initial geometries. Several isomers, with slightly different energies, are found within a ~35% energy range of the lowest energy isomer. Isomers with approximately the same energy can have a different structure. The structures of the three isomers indicated in the histogram are shown in the Supporting Information (Figure S2).

stable one—the dimer structure is maintained, but its orientation with respect to the molecule is different. At somewhat higher energies, the AN dimer is oriented differently with respect to the aromatic molecule, and only at still higher energies (~2 kcal/mol above the most stable structure), isomers in which the two AN molecules are separated from each other were obtained. Figure S2 (in the Supporting Information) shows the structures of some of those higher energy isomers: In the case of PP:AN$_2$, each AN lies at opposite sides of the molecule, whereas, in the case of PBN:AN$_2$, one of the AN stays close to the aromatic ring (benzene or pyrrole) and the other near the cyano group.

*(3) Clusters of Ground-State PP or PBN with Three AN Molecules.* Numerous minima were found for clusters with more than two AN molecules; their binding energies were often found to be very similar. A close inspection reveals that a clear structural pattern is repeated in these clusters with slight energy and geometry variations. Five and six different minima were found to lie within a 4% energy range of the lowest energy isomer for PP:AN$_3$ and PBN:AN$_3$, respectively. The barriers between various equilibrium conformations are quite small due to the weak van der Waals interactions between the molecules. Therefore, the cluster structures are not rigid and rapid transitions between them can take place even at low temperatures.[32] The lowest lying structures (and their corresponding energies) are shown in Figures S3 and S4 (Supporting Information) for PP and PBN, respectively. In all of these minima, the three AN molecules are located on the same side of the molecule (of the benzene ring plane, to be more precise).

In the three lowest energy PP:AN$_3$ isomers, the acetonitrile trimer has a "T" shape structure which can be viewed as consisting of a dimer and a monomer. In PP:AN$_3$(I), the dimer is located above the PP molecule approximately as in the PP:AN$_2$(I) cluster (therefore strongly interacting with the molecule), whereas the third AN molecule interacts only with the dimer (electrostatic interaction between the methyl and the cyano groups). The two other isomers differ chiefly by the orientation of the acetonitrile trimer with respect to the PP molecule. In the PP:AN$_3$(IV) isomer, the AN molecules are arranged in an alternating head to tail configuration. Two of the AN molecules are located as in the PP:AN$_2$(I) cluster, and the third one interacts with another AN. In PP:AN$_3$(V), the three acetonitrile molecules
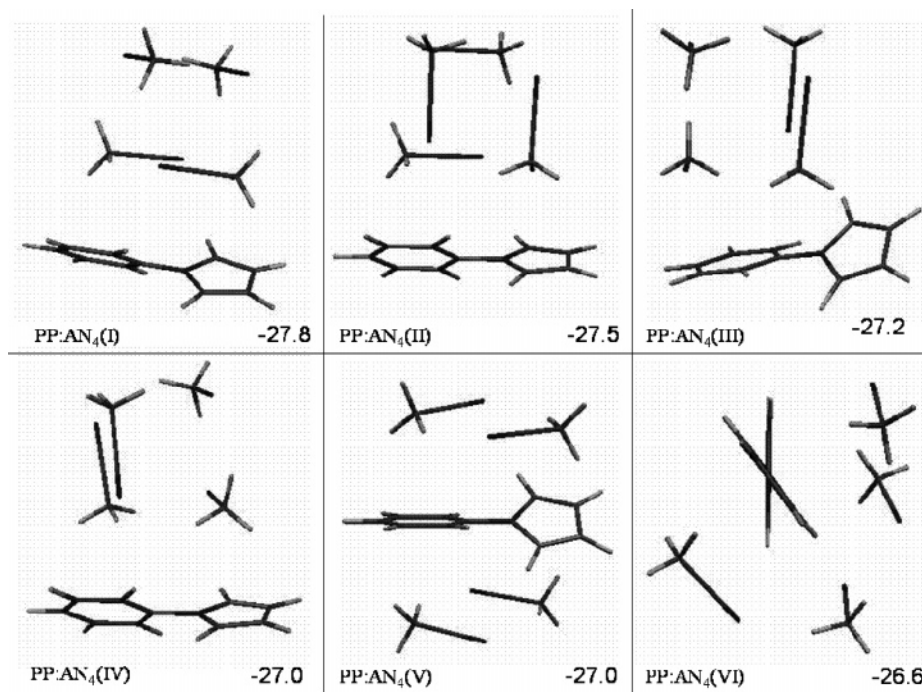
**Figure 5.** Structures of the six lowest energy isomers of the PP:AN$_4$ cluster. The notation (left) and binding energy in kilocalories per mole (right) are indicated below the sketch of each isomer.

are also arranged in a 2 + 1 configuration. But, in this case, one molecule from the AN dimer interacts with the benzene ring of PP and the monomer interacts with the pyrrole ring. It can be noticed that, in all of the PP:AN$_3$ clusters, one of the AN molecules is attached mainly to the other(s) rather than to the PP molecule.

In the most stable PBN:AN$_3$(I) isomer, the acetonitrile trimer also consists of a dimer (located above PBN as in PBN:AN$_2$) and a monomer close to the cyano group. The AN monomer interacts more strongly with the aromatic molecule in the case of PBN than in the case of PP (possibly due to stronger dipole—dipole interaction). This is manifested by the larger energy difference between the PBN:AN$_n$(I) and PP:AN$_n$(I) clusters for $n$ = 3 (1.1 kcal/mol) than for $n$ = 2 (0.5 kcal/mol). In PBN:AN$_3$(II), the acetonitrile trimer is located above the benzonitrile moiety, in a 2 + 1 configuration in which the monomer interacts with the cyano group of PBN, whereas an AN molecule from the dimer interacts with the benzene ring. The third AN molecule is attached to the other AN molecules. The PBN:AN$_3$(III) isomer is similar to PBN:AN$_3$(I) except that the two paired AN molecules are not strictly parallel to each other and the monomer is closer to the other AN pair than in PBN:AN$_3$(I). The PBN:AN$_3$(IV) structure is the most symmetric one: Two AN ligands are located in the plane of the benzene ring, one on each side of the ring, and oriented such that the methyl groups point toward the cyano group of PBN, and the third AN ligand is parallel to the molecular axis, in the opposite direction. In the PBN:AN$_3$(V) isomer, the AN molecules consist of a 2 + 1 "T" shape structure close to the benzonitrile moiety. Finally, the acetonitrile trimer in PBN:AN$_3$(VI) forms an alternating head to tail configuration in which the methyl group of the middle AN is above the benzene ring.

*(4) Clusters of Ground-State PP or PBN with Four AN Molecules.* For PP:AN$_4$ and PBN:AN$_4$, six and seven different isomers were found respectively within a 5% energy range of the lowest energy isomer, as shown in Figure 5 and Figure 6. In the four lowest energy PP:AN$_4$ structures, the four AN molecules form the energetically most stable tetramer. The

binding energy between the AN molecules in the most stable isomer PP:AN$_4$(I) (−19.5 kcal/mol) is very close to the energy reported for the minimum structure of AN$_4$ (−19.8 kcal/mol for the same parameters),[30] indicating that the presence of the PP molecule hardly alters this structure. In that isomer, only one of the two AN pairs is directly attached to the molecule (and oriented as in the PP:AN$_2$(I) isomer), whereas in the PP:AN$_4$(II), PP:AN$_4$(III), and PP:AN$_4$(IV) isomers the molecule is attached to both AN pairs. The isomer PP:AN$_4$(V) consists of two AN pairs, one on each side of the PP molecule, and is attached as in PP:AN$_2$(I). In the PP:AN$_4$(VI) isomer, three of the AN molecules are located on one side of the benzene plane, exactly as in the PP:AN$_3$(IV) isomer, and the AN located on the other side of the plane is attached to the pyrrole ring.

In the most stable PBN:AN$_4$(I) structure, the AN tetramer consists of two pairs, one located above the molecule (as in PBN:AN$_2$) and the second attached approximately at a right angle to the first. In contrast with PP:AN$_4$(I), the AN molecules of the second pair interacts also with the larger molecule (methyl group of AN with the cyano group of PBN). In the PBN:AN$_4$(II) isomer, the AN tetramer exhibits a cyclic structure similar to the unit cell of the monocyclic phase of acetonitrile.[33] However, the symmetry of this structure (with respect to the inversion center) is broken by the interaction with the PBN molecule: the AN ligand close to the cyano group is closer to the plane of the benzene ring than the other ligands. The two next higher energy isomers (very close in energy) have the AN molecules arranged as two dimers, located on the same side of the molecule. One of the AN pairs is attached to the aromatic rings, and the second pair is approximately at right angles to the first one in PBN:AN$_4$(III), whereas it is parallel to the first one in PBN:AN$_4$(IV). In those two isomers, the cyano group of PBN is attached to the methyl group of the nearest AN molecule. The PBN:AN$_4$(V) isomer resembles PBN:AN$_3$(IV) in the way two of the AN molecules are oriented with respect to the cyano group of PBN. The two other AN molecules form a dimer located above the benzene ring. In PBN:AN$_4$(VI), the four AN molecules are close to the benzonitrile moiety and form
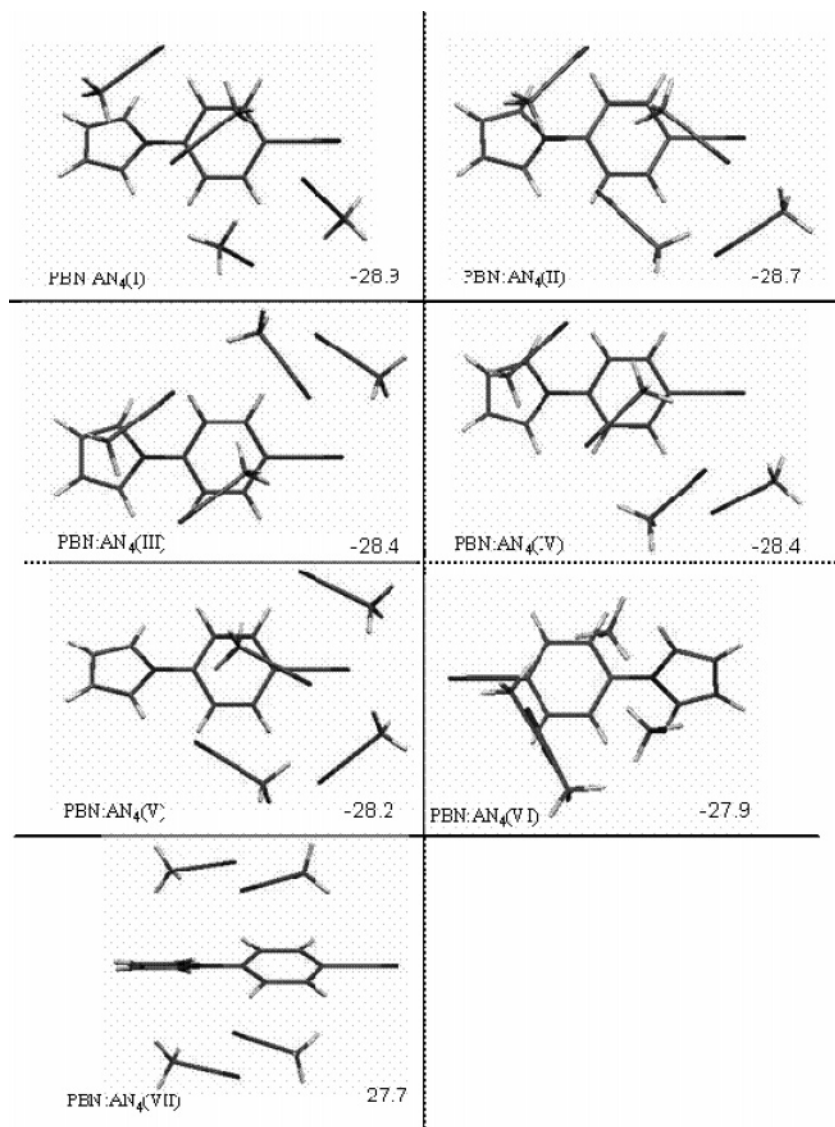
Photophysics of Phenylpyrrole Derivatives

*J. Phys. Chem. A, Vol. 109, No. 17, 2005* **3835**



**Figure 6.** Structures of the seven lowest energy isomers of the PBN:AN$_4$ cluster. The notation (left) and binding energy in kilocalories per mole (right) are indicated below the sketch of each isomer.

the stable tetramer. Finally, the isomer PBN:AN$_4$(VII) consists of an AN pair on each side of the molecule, as in PP:AN$_4$(V).

*(5) Clusters of Ground-State PP or PBN with More Than Four AN Molecules.* In clusters of PP with five or more AN molecules, a large number of clusters with similar binding energies were obtained. The most stable structure (BE = −34 kcal/mol) can be viewed as the PP:AN$_4$(VI) isomer in which an added AN molecule forms a dimer with the unpaired AN attached to the pyrrole ring: the AN ligands of the lowest energy isomers lie on both sides of the phenyl ring plane. One stable isomer (BE = −33 kcal/mol) has three AN molecules on one side (located as in PP:AN$_3$(I)) and two AN molecules on the other side of PP (located as in PP:AN$_2$(I)). Still another isomer with the same binding energy (BE = −33 kcal/mol) has all five AN molecules on the same side of the molecule. In the most stable PP:AN$_6$ cluster, the ligands wrap around the PP molecule: Two ligands are located as in the PP:AN$_2$(I) cluster, a third one is found at a right angle with the AN pair, and two others are approximately parallel to the latter (one roughly in the plane of the benzene ring and the second close to the pyrrole ring). In contrast with the smaller clusters, clusters of this size and larger having drastically different structures were found to lie within a narrow energy range. In view of these results, the

detailed study of large-cluster structures was discontinued—it is more appropriate to discuss the distribution properties for these larger clusters, rather than the small differences.

In the most stable PBN:AN$_5$ isomer, all the AN ligands lie on the same side of the PBN molecule and are located preferentially in proximity to the cyano group (three of them form a structure reminiscent of the PBN:AN$_3$(IV) isomer). This pattern is repeated also in the most stable PBN:AN$_6$ isomer: the AN ligands are found on the same side of the molecule. The structure thus formed may be viewed as the PBN:AN$_4$(V) isomer to which an AN dimer has been added on the pyrrole side. Higher energy isomers (of PBN:AN$_5$ and PBN:AN$_6$) have AN ligands on both sides of PBN. Since six AN molecules can be placed as nearest neighbors on each side of PBN, the first solvation layer of PBN can include at least 12 AN molecules. In contrast, a similar argument shows that the first solvation layer of PP can consist of only eight AN molecules. The binding energies of the most stable ground-state clusters of PP and PBN with acetonitrile (up to 6 AN molecules) obtained from the MM calculation are collected in Table 3. The table also reports the partition of the total stabilization energy to contributions from AN−AN interactions compared to interactions between the pyrrole derivative and AN molecules. The partition is based on

**3836** *J. Phys. Chem. A, Vol. 109, No. 17, 2005*

Schweke et al.

**TABLE 3: Total Binding Energies (kcal/mol) of the Most Stable Clusters of PP and PBN in the Ground State with *n* AN Molecules, *n* = 1−6** [a]

| | GS PBN:AN$_n$ | | | GS PP:AN$_n$ | | |
|---|---|---|---|---|---|---|
| *n* | $E_{total}$ | $E_{AN-AN}$ | $E_{PBN-AN}$ | $E_{total}$ | $E_{AN-AN}$ | $E_{PP-AN}$ |
| 1 | −5.3 | | *−5.3* | −5.1 | | *−5.1* |
| 2 | −14.0 | −5.5 | *−8.5* | −13.6 | −5.5 | *−8.1* |
| 3 | −20.5 | −7.5 | *−13.0* | −19.4 | −10.3 | *−9.1* |
| 4 | −28.9 | −15.2 | *−13.7* | −27.8 | −19.5 | *−8.3* |
| 5 | −35.4 | −18.8 | *−16.6* | −34.0 | −19.7 | *−14.3* |
| 6 | −43.8 | −25.6 | *−18.2* | −41.5 | −24.5 | *−17.0* |

[a] The partition of the total energy to the contributions from the interaction between the AN molecules $E_{AN-AN}$ and the interaction between PP or PBN and the AN ligands is also listed (in columns 4 and 7 in italics). Data are from MM calculations.
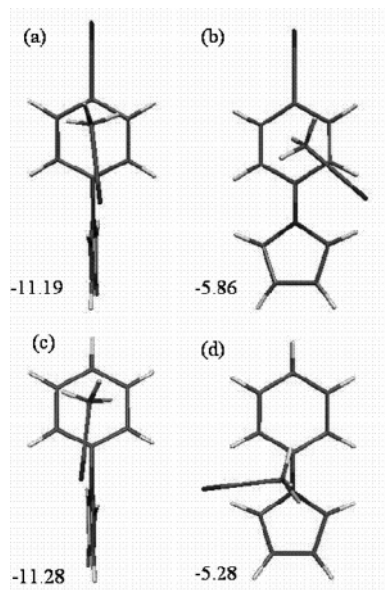


**Figure 7.** Structures of the most stable isomers of PBN:AN (top) and PP:AN (bottom) 1:1 clusters in the excited CT states. (a and c) Phenylpyrrol derivative in the antiquinoid (AQ) minimum. (b and d) Phenylpyrrol derivative in the quinoid (Q) minimum.

the assumption that all interactions between the constituents of the cluster are of pairwise nature only.

*(6) Acetonitrile Clusters of Excited States of PP or PBN.* The charge distribution of the pyrrolobenzene derivatives is significantly altered when passing from the ground state to either of the CT states minima: the AQ form (twisted) or the Q one (planar). As a result, the geometries of the ground-state clusters are quite different from those of the CT state clusters, for both PP and PBN. The calculated geometries of the 1:1 clusters are shown in Figure 7. They can be readily accounted for on the basis of the charge distribution shown in Figure S1 of the Supporting Information. The AQ structures have high dipole moments (10.6 and 16.4 D for PP and PBN, respectively). In both molecules, the total negative charge (summed on heavy atoms) is higher on the phenyl ring than on the pyrrole ring (in contrast to the GS). Therefore, in both clusters, the AN axis lies in the same plane as the benzopyrrole axis and the AN methyl group is located above the phenyl ring. In the Q form of PP, a high negative charge is concentrated on the carbon atoms close to the central C−N axis. The most stable cluster is thus obtained when the CN bond of acetonitrile lies perpendicularly to the molecular axis of PP with the methyl hydrogen atoms pointing toward the two rings. In the Q form of PBN, a high negative charge is concentrated on the π system

**TABLE 4: Total Binding Energies (kcal/mol) of the Most Stable Clusters of PP and PBN in the Charge-Transfer-State AQ Minimum, with *n* AN Molecules, *n* = 1−5** [a]

| | AQ PBN:AN$_n$ | | | AQ PP:AN$_n$ | | |
|---|---|---|---|---|---|---|
| *n* | $E_{total}$ | $E_{AN-AN}$ | $E_{PBN-AN}$ | $E_{total}$ | $E_{AN-AN}$ | $E_{PP-AN}$ |
| 1 | −11.2 | | *−11.2* | −11.3 | | *−11.3* |
| 2 | −21.8 | 0.6 | *−22.4* | −22.0 | 0.6 | *−22.6* |
| 3 | −29.4 | 0.3 | *−29.7* | −29.5 | 0.4 | *−29.9* |
| 4 | −38.6 | −4.6 | *−34.0* | −36.7 | −4.7 | *−32.1* |
| 5 | −45.4 | −4.5 | *−40.9* | −44.2 | −11.7 | *−32.6* |

[a] Data are from MM calculations; notations, as in the footnote of Table 3.

(−0.82 e) of benzene. As a result, the optimized position of the AN ligand is such that the methyl group lies above the electronic cloud of the ring and the nitrile group interacts with the closest hydrogen atoms. The most stable clusters of PP and PBN in the excited AQ form with *n* AN molecules (*n* = 2−4) are shown in Figure S5 of the Supporting Information, and the energies (*n* = 1−5) are listed in Table 4. In contrast to the GS case, the structures of these clusters are very similar for PP and PBN. In the optimized geometry obtained with 2 AN ligands, one AN molecule lies on each side of the benzene ring and is oriented as in the 1:1 cluster. The resulting energy is twice the 1:1 cluster binding energy (∼−22 kcal/mol). It is noted that this structure differs from the corresponding GS cluster in which the two AN molecules lie on the same side of the pyrrole derivative and formed a dimer. In the AQ−PP:AN$_3$ and AQ−PBN:AN$_3$ clusters, two AN ligands are oriented nearly as in the AQ−PP:AN$_2$ or AQ−PBN:AN$_2$ clusters, whereas the third one interacts with both the aromatic molecule and with one of the other AN ligands. The two latter clusters of PP and PBN differ slightly in the position of this third ligand molecule. In the clusters of PP and PBN with 4 AN molecules, one molecule is located on one side of the benzene ring, whereas the 3 others are located on the other side of the ring.

For *n* = 5, the geometry difference between the most stable clusters of PP and PBN becomes more apparent: whereas, in the PP cluster, the fifth AN molecule interacts mostly with the ligands surrounding the molecule, in the PBN cluster, the fifth AN molecule is attached to PBN at the cyano group.

**(B) Argon Matrix Trapping Sites.** A trapping site characterizes the variation in the structure of the rare-gas matrix in the vicinity of the trapped molecule. In general, trapping sites for polyatomic molecules differ by the cavity size (the number of argon atoms removed from the full fcc lattice) and by the displacement of the remaining atoms from their perfect lattice position. In this study we shall consider mainly the cavity size, which for large nonplanar molecules is expected to be the major discriminating factor between different trapping sites. Figure 8 introduces the format chosen for representing different trapping sites. The two {001} layers in which the trapped molecule replaces argon atoms are shown in different colors and are displayed in two different projections (along the *x*−*z* and *x*−*y* planes). The geometry of the cavity formed by the "removed" argon atoms is shown in the center. The "missing" argon atoms are shown inside the corresponding boundary box, whose limits are directed along the 001 axis. A space-filled model of the removed argon atoms is also shown.

*(1) Isolated PP and PBN Molecules.* For PP and for PBN in argon, 54 deposition runs were completed. The resulting sites consisted of cavities in which 5−7 argon atoms were replaced by PP and 6−8 atoms by PBN. For both molecules, the 6-substitutional site (SS) was the most frequently encountered one. The relative probabilities for the attainment of different-
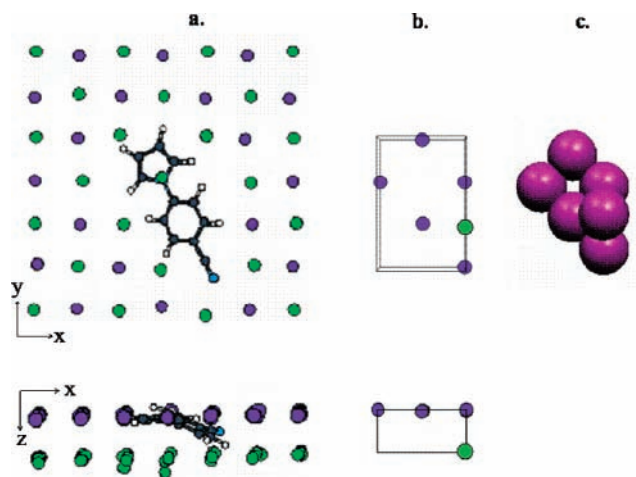
Photophysics of Phenylpyrrole Derivatives

*J. Phys. Chem. A, Vol. 109, No. 17, 2005* **3837**



**Figure 8.** Three alternative ways for presenting the structure of a trapping site of PBN. (a) Overlay of the two {001} layers (shown in different colors) in which the molecule replaces argon atoms represented in two different projections (along the $x-z$ and $x-y$ planes). (b) Simplified presentation of the cavity's geometry: The "missing" atoms are shown inside the corresponding boundary box, whose limits are directed along $x-y$ or $x-z$ planes. (c) More compact presentation using a space-filled model composed of the argon atoms removed from the matrix.

**TABLE 5: Relative Probabilities of Trapping in an *n*-Substitutional Site (*n* Argon Atoms Removed from the Perfect fcc Lattice of an Argon Crystal) for PP and PBN***[a]*

| | % of runs | |
|---|---|---|
| argon atoms replaced | PP | PBN |
| 5 | 24 | |
| 6 | 67 | 74 |
| 7 | 9 | 22 |
| 8 | | 4 |

*[a]* 54 different runs were done for each molecule.

sized substitutional sites are listed in Table 5. The relative probabilities of formation of a trapping site are equated to the percentage of runs leading to it.

The smallest trapping site of PBN in argon is 6 substitutional (smaller sites cannot accommodate PBN because of strong repulsion forces). In the most stable site (6a), the molecule replaces 6 argon atoms in the {111} plane. In sites 6b and 6c, the molecule replaces 5 argon atoms in one {001} plane and one atom in an adjacent plane. These two sites of nearly equal stabilization energy differ by the position of this argon atom relative to the five others. In previous studies of aromatic molecules,[27,34] the trapped molecule was planar and therefore all missing argon atoms originated from the same lattice plane. The different end result in the case of PBN is due to its lower symmetry ($C_2$). The distortion caused to the surrounding matrix atoms is significantly larger when the molecule occupies mainly a {001} plane, as in site 6b, than a {111} plane, as in site 6a. This can be seen in Figure 9 that shows the geometry of sites 6a and 6b. Figure 10a shows the cavities of the three most stable trapping sites of PBN.

In the case of PP (see Figure 10b), the smallest possible site is obtained by the replacement of 5 atoms from the {111} plane of the crystalline argon (site 5a). This is the energetically most stable trapping site for PP, but not the most frequently encountered one. For this site a large distortion of the lattice was recorded. In the more frequently attained sites, the molecule replaces 6 argon atoms in two possible geometries: either 6 atoms are replaced from the {111} plane (site 6a) or 5 atoms
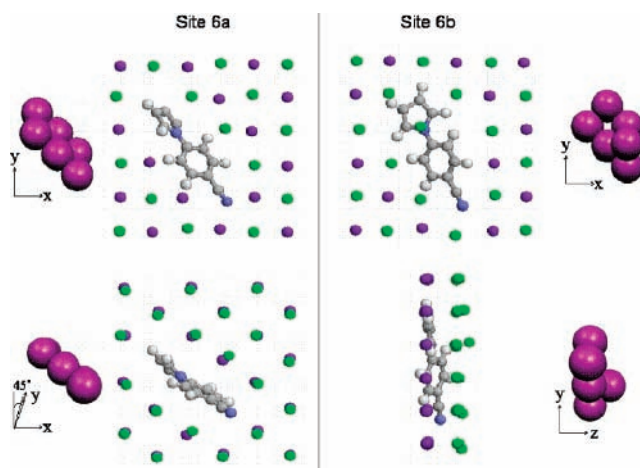


**Figure 9.** Structures of two different trapping sites of PBN, site 6a (left) and site 6b (right). Top: Overlay of the two {001} layers in which the molecule replaces argon atoms with the corresponding space-filled model of the "missing" atoms. Bottom: Space-filled models of the trapping sites.

are removed from the {001} plane and an additional one is removed from the adjacent {001} plane (site 6b). In this particular site, the molecule can accommodate itself in various ways. For example, either the benzene ring or the pyrrole ring can lie in the main {001} plane.

*(2) Trapping Sites for 1:1 Clusters of PP with AN.* Acetonitrile deposited in an argon matrix was found to occupy a two substitutional site in which the molecule is oriented along the {111} axis, as shown in Figure S7 of the Supporting Information (12 runs were made; all led to this site). The smallest trapping sites found for the GS−PP:AN(I) cluster may be viewed as a PP molecule trapping site from which two additional argon atoms were removed. The structures of some of these sites are shown in Figure 11a. The number of different possible 7-substitutional site structures was rather high, with only small structural variations between them: the two additional missing argon atoms (in light gray) are located inside the same boundary box. Bigger cavities of higher energies were also recorded in which the cluster replaces up to 10 argon atoms.

The trapping sites for clusters of PP in the AQ form (90° twisted) with AN can also be considered as trapping sites of twisted PP with two additional missing atoms. A set of 25 runs for simulating the sites of the isolated PP molecule in the AQ geometry in argon was completed. The number of atoms replaced by this molecule varied between 5 and 7 (as for the ground state of PP), but the occurrence of the 7 SS was the highest (56% compared to 22% for both the 5 SS and the 6 SS). Numerous different sites, in which the missing atoms are distributed among two or three planes, were also obtained. These results indicate that the trapping sites for the twisted form of PP are bigger than those for the GS molecule. It can also be concluded that the number of possible sites increases significantly as the geometry of the trapped molecule differs from planarity, all the more so for asymmetric clusters. The clusters of twisted PP with AN occupy cavities of 8−11 argon atoms. The most stable cavities are displayed in Figure 11b. These trapping sites are different (and usually bigger) from those of the ground-state PP:AN cluster. But the limits of the boundary box are, in most cases, identical for the GS PP:AN and the AQ PP:AN clusters.

The sites of PP in the Q geometry (planar) with AN were also simulated (31 runs). In this case, the distribution of sites was much narrower than for the AQ form. In more than 80%
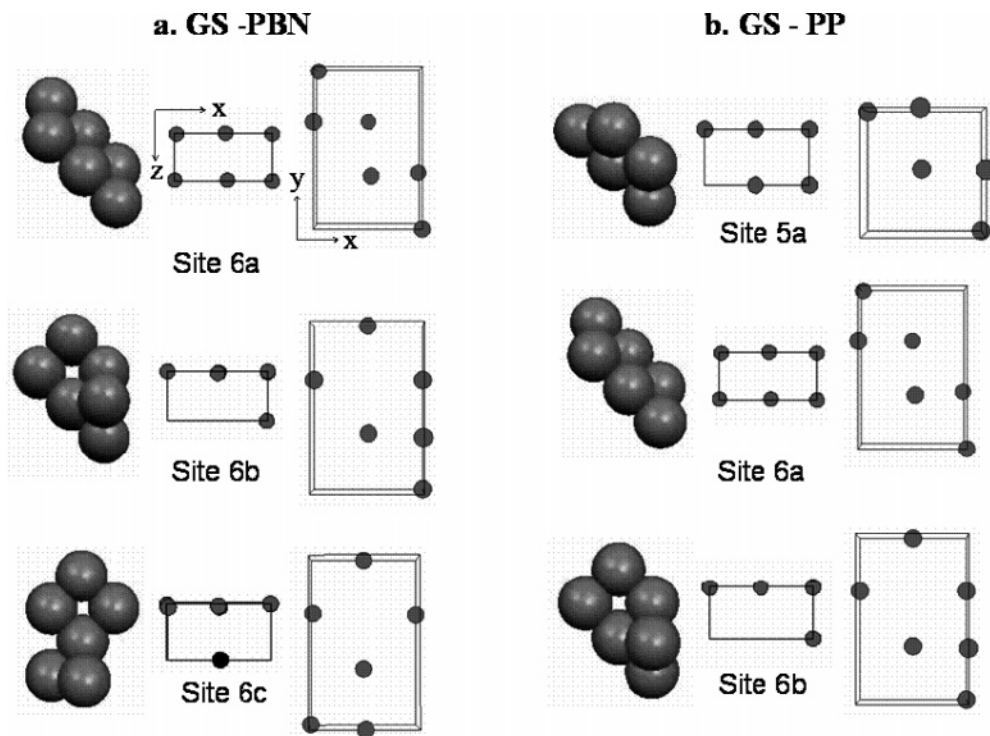
**a. GS -PBN**

**b. GS - PP**



**Figure 10.** Structures of the three most stable cavities of PP (right) and PBN (left) trapped in an argon matrix. Each cavity is represented by the space-filled model and by the corresponding boundary box shown in two different projections.
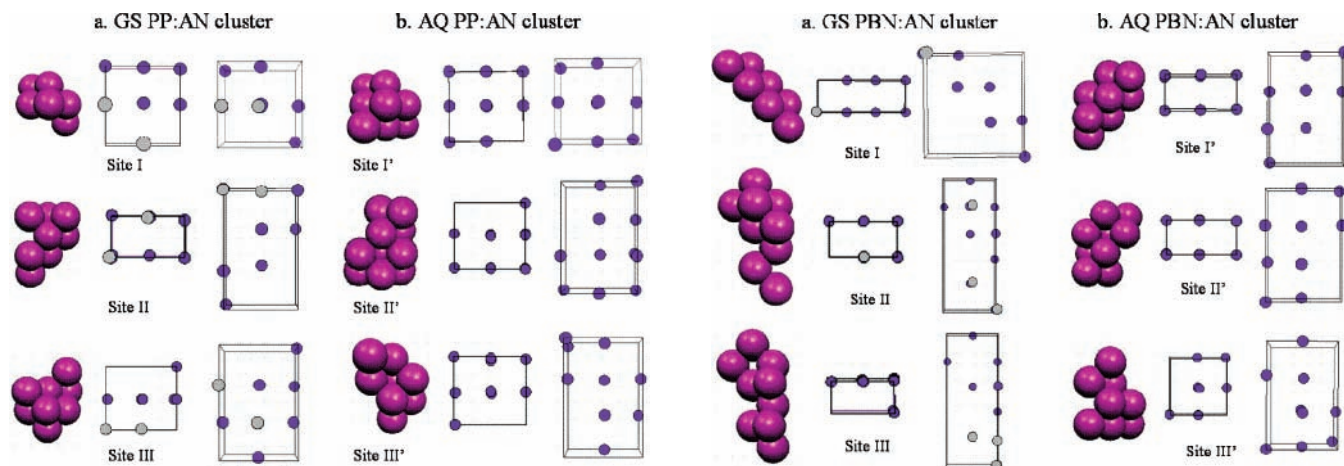


**Figure 11.** (a) Examples of cavities of the ground-state PP:AN cluster trapped in an argon matrix. Argon atoms missing in the trapping site of the isolated molecule are painted blue; the gray ones are additional atoms removed upon the insertion of AN. (b) Examples of cavities in an argon matrix of the AQ PP:AN cluster. See Figure 8 for explanation of the representations.

of the runs, the molecule was located in the {111} plane and two additional atoms (in a few cases only one) were removed from the adjacent plane, along a {111} axis. The structure of this site is thus identical to that of site II of the stable GS–PP:AN cluster. In the other runs, the molecule was located in the {001} plane and the resulting cavities consisted of 10 or 11 missing atoms. It appears that when the PP molecule lies in the {001} plane, the AN ligand cannot be oriented along the {111} axis (which is, as mentioned above, the only stable site for AN). The fact that the AN molecule cannot be placed in its "natural" trapping site explains the abundance of big cavities in the case of this cluster.

*(3) Trapping Sites of 1:1 Clusters of PBN with AN.* The smallest cavities for the PBN:AN cluster in argon consist of
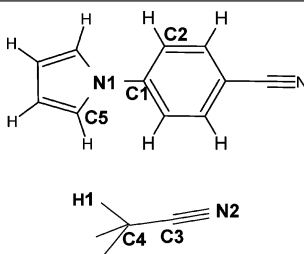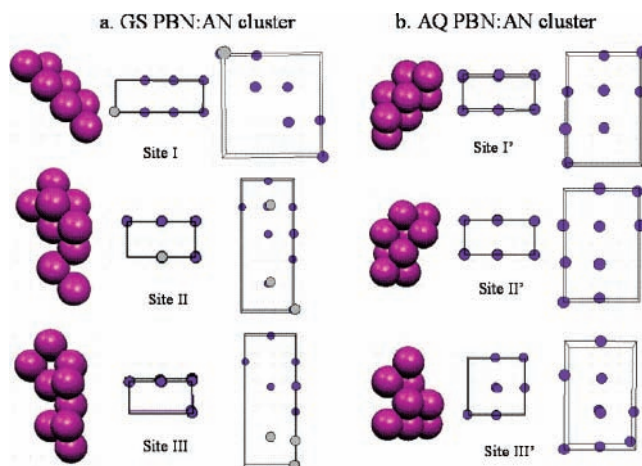


**Figure 12.** (a) Examples of cavities of the ground-state PBN:AN cluster trapped in an argon matrix. (b) Examples of cavities in an argon matrix of the AQ PBN:AN cluster. See Figures 8 and 11 for notation.

7–11 missing atoms, 6 of which are located as in PBN sites. The most stable cavities are shown in Figure 12a. In the 7 SS site, the distortion of the crystalline structure is significant and extends to the third surrounding layer. The fact that the AN molecule lies in proximity to the cyano group of PBN in this cluster induces the removal of one or two additional argon atoms along the longer axis of the cavity ({111} axis for site I or (001) axis for sites II and III).

The clusters with PBN in its AQ geometry occupy sites of 9–11 argon atoms (see Figure 12b). The cavity structures are rather similar to those of twisted PP with AN. This result is consistent with the fact that the cluster geometries of AQ–PP:AN and AQ–PBN:AN clusters are nearly identical. It is important to notice that, in contrast to the case of PP, the dimensions of the boundary box are different for GS–PBN:AN clusters and AQ–PBN:AN ones.

Photophysics of Phenylpyrrole Derivatives

*J. Phys. Chem. A, Vol. 109, No. 17, 2005* **3839**

**TABLE 6: Comparison of the Most Stable Cluster Structure for PP:AN and PBN:AN Clusters, Obtained with DFT (B3LYP/aug-cc-pVDZ) and MM Calculations**[a]

| | PP:AN | | PBN:AN | |
|---|---|---|---|---|
| | MM | DFT | MM | DFT |
| $N_2-C_1$ (Å) | 4.5 | 4.5 | 6.1 | 5.9 |
| $N_2-C_1-N_1$ (deg) | 73.2 | 75.4 | 138.3 | 138.6 |
| $N_2-C_1-N_1-C_5$ (deg) | 56.6 | 55.9 | 25.6 | 28.7 |
| $C_3-N_2-C_1$ (deg) | 64.9 | 78.5 | 110.5 | 121.1 |
| $N_2-C_3-C_1-N_1$ (deg) | 50.6 | 45.5 | 2.4 | 2.7 |
| $H_1-C_4-N_2-C_1$ (deg) | 34.3 | 32.8 | 56.1 | 42.7 |

[a] The indexes on the atoms refer to those indicated in the picture.

## IV. Discussion

In the first part of this section the results for the 1:1 cluster structures and energies obtained by the two methods (DFT and MM) are compared. In the second part, the implications of these results on the interpretation of the experimental data obtained in supersonic jets and in cryogenic matrixes are considered.

**(A) Comparison of Quantum Chemical and MM Results.** For both PP and PBN molecules, the agreement between cluster geometries from the quantum chemical calculation and those obtained from the MM calculation was very good. Table 6 compares the calculated cluster geometries by the use of six intermolecular parameters describing the position of the AN ligand relative to the pyrrolo derivative. Examination of the data leads to the following conclusions: (1) For both PP and PBN, the position of the AN nitrogen relative to the pyrrolo derivative is in good agreement in the two calculations. (2) The main difference in the calculated geometries of the PP:AN cluster is the orientation of the AN axis relative to the PP molecule. (3) The differences between the calculated PBN:AN structures are found in the position of the methyl hydrogen atoms relative to the plane of the benzene ring.

The energies of the optimized structures obtained from the MM calculation are listed in Table 3. According to the DFT calculation, the binding energy of the PBN:AN cluster is bigger by ~2 kcal/mol than that of the PP:AN one. In contrast, the binding energies for the two clusters are very close according to the MM optimization algorithm. This may indicate that the MM calculation overestimates the interaction between PP and the AN ligand or the inadequacy of the level of theory (B3LYP functional) and the basis set (aug-cc-pVDZ) used in the DFT calculation. The attractive force between PBN and AN is mainly electrostatic, but in the PP:AN cluster it is due to both electrostatic and dispersive contributions. To reproduce the dispersion interaction, electron correlation must necessarily be included in the calculation. Although DFT includes some electron correlation, it fails to reproduce the dispersion interaction.[35,36] The fact that the binding energies in the PP:AN and PBN:AN clusters are very similar according to the HF-MP2/cc-pVDZ calculation also indicates that the dispersion contribution is underestimated by the DFT calculation. Further support for this conclusion can be gained by considering the binding energies reported for related clusters, for instance, the benzene:AN one[31] (−3.70 kcal/mol). Since the most stable isomer of PP:AN consists of AN above the pyrrole ring (and not above the benzene one), a stronger intermolecular force is expected in the PP:AN cluster than in the benzene:AN one, which means that the binding energy in PP:AN must be higher than −3.70 kcal/mol.

It is therefore concluded from the comparison between the MM and DFT calculations that the MM procedure succeeds in predicting the cluster structure and yields a reasonable estimate of the binding energy. It is probably better adapted to reproduce the dispersion interaction than the DFT calculation.

**(B) Interpretation of the Jet Results.** The differences between the binding characteristics of the AN clusters of PP and PBN can help to settle the problem put forward in the Introduction: Why is CT emission observed from clusters of PBN with AN ($n \geq 4$) composed of two separate bands, whereas emission from clusters of PP with AN of any size consists of a single band? In the gas phase, the LE state is lower in energy than the CT state. Solvation of the pyrollobenzene derivative by polar molecules may create a van der Waals (vdW) cluster in which the CT state is lower in energy (at its optimum geometry) than the LE state. This is a necessary condition for the observation of CT emission, but not a sufficient one. It is necessary to consider also the dynamics of the electronically excited system, in particular possible competing processes.

In small ($n = 1, 2$) clusters of benzene with hydrogen-bonding molecules (such as $H_2O$,[37] $CH_3OH$,[38] and $CHCl_3$ [39]) or acetonitrile,[31] a blue-shift is observed in the electronic transition, indicating a decrease in the binding energy of the cluster following the excitation. These experimental observations refer to the $1^1B_{2u} \leftrightarrow 1^1A_{1g}$ transition of benzene. Recalling the covalent nature of the $1^1B_{2u}$ state, the behavior is expected to be different for the transition to the A state of the pyrrolobenzene derivative (derived from the $1^1B_{1u}$ state of benzene) due to the ionic nature of this state. The MM calculation (Tables 3 and 4) indicates that the binding energy in both PP:$AN_n$ and PBN:$AN_n$ clusters increases upon electronic excitation of the chromophore to form the CT−AQ state. The binding characteristics of these molecules in the LE state to AN in a cluster is expected to be similar to that of the ground state (GS).

In order for CT emission to be observed in jet-cooled clusters, at least three conditions must be satisfied. The energy of the CT state must be lower than that of the LE state, the rate of conversion of the LE state to the CT one must be greater than competing processes such as fluorescence, intersystem crossing (ISC) to the triplet, and vibrational predissociation (VP) releasing one or more ligands. In addition emission from the CT state must compete favorably with other energy dissipation processes.

The calculations summarized in Tables 3 and 4 show that the total binding energy of the AQ M:$AN_n$ clusters is larger by about 10 kcal/mol than in the GS M:$AN_n$ for a given $n$ (M = PP or PBN). By assumption, this is also the difference between the BEs of the LE and AQ states and appears to be sufficient to lower the AQ state to below the LE state. Previous time-resolved experiments have shown that there is a correlation

between the VP rate and the number of vdW modes:[40,41] An increasing number of vdW modes slows down the VP rate, as expected from a statistical model. Typical VP rates were found to be on the order of $>10^9$ s$^{-1}$ at a few hundred cm$^{-1}$ above the dissociation threshold for small clusters. These rates are larger than the observed fluorescence decay rates of PP:AN and PBN:AN clusters in jets[3,4] ($\sim10^8$ s$^{-1}$ for the LE state, $4 \times 10^7$ s$^{-1}$ for the CT state of PBN). Thus, VP rates are large enough to allow dissociation of an LE cluster in competition with LE→CT transition. According to the analysis of the data of the Table 3, if the energy excess in the nascent cluster is large enough, it may lead to the ejection of a whole AN$_4$ cluster from the PP cluster, whereas in the case of PBN, only one AN molecule will be ejected, the remaining PBN:AN$_3$ cluster being sufficiently stabilized to reach the bottom of its potential surface and eventually fluoresce leading to the observed LE emission band.

In the case of larger clusters of PP with AN ($n > 5$), however, our calculation shows that the CT state is sufficiently stabilized and that the transition from the LE state to the CT one is probable upon ejection of one or more AN molecules. The observation of only one band may be due to the fact that the AQ−CT emission in this case is from vibrationally excited CT clusters, and thus not spectrally resolved from the LE emission. Inspection of the spectra shows that the band is broader when the fraction of large clusters increases.[4] This point warrants further experimental work.

Analysis of the PBN cluster structures also rationalizes the experimental observations that the excitation spectra of the red (CT) band and of the [PBN(AN)$_n$]$^+$ mass peaks ($n = 0$−5) are completely devoid of vibrational structure.[4] The coexistence of a large number of closely spaced minima, leads to spectral congestion which prevents the observation of vibrational structure in the excitation spectrum, in contrast to the case of the bare molecule.[3] Furthermore, as the barriers between several minima are expected to be very small, a cluster of a given composition can deform from one minimum energy conformation to another even at the low-temperature prevailing in the jet. Each cluster finds itself in a shallow potential well, allowing the execution of large-amplitude vibrations. The two effects combine to generate a large number of close-lying transitions, resulting in a broadened absorption band.

**(C) Interpretation of the Matrix Isolation Results.** *(1) Neat Argon Matrixes.* In neat argon, PBN shows both LE and CT emissions, whereas PP exhibits only the LE one. The energy gap between the B and A states of the isolated molecules ($\Delta E$), determined in supersonic expansion at the Franck−Condon region, cannot explain this different behavior since $\Delta E$ is very similar in PBN and PP (450 and 500 cm$^{-1}$, respectively).[3] QC calculations[13] predict that in both isolated molecules the lowest energy CT minimum is the quinoid form (Q). But this form has a very different dipole moment in PP (0.8 D) and PBN (11.0 D). The polarizable nature of the matrix medium leads to a stabilization of the trapped species, which is larger for the ionic excited state. In the case of PP, the Q form has approximately the same dipole moment as the GS so there is no ordering reversal: the LE state remains the lowest excited state in solid argon. In contrast, in the case of PBN, the Q state (which can be formed with only little perturbation in the matrix) has a significantly higher dipole moment than the GS and becomes slightly lower than the LE state in argon.[10] The AQ state (maybe in a partially twisted structure) can also be stabilized and contribute to the CT emission band. Emission from both LE and CT states is thus expected to be observed.

The nature of the CT state in argon matrixes is discussed in more detail in section IV(C)(3).

*(2) AN-Doped Argon Matrixes.* Experimentally, addition of AN to the argon matrix leads to the appearance of a new, well-separated emission band in the case of PP, whereas the emission spectrum of PBN is not significantly altered. A statistical distribution of the AN molecules in argon predicts that, for an AN/argon ratio of 1/100, each pyrrolo derivative has on average less than one AN nearest neighbor.[9] Therefore only 1:1 clusters need to be considered for interpreting the experimental results in the argon matrix doped by 1% AN. AN clusters with PP or PBN are not formed at room temperature; the deposition is carried out separately for the two species: However, a pyrrolo derivative reaching the argon matrix in the vicinity of a previously deposited AN molecule which is still lying on the surface is likely to attach to it. Successive collisions with other argon atoms are likely to locally anneal the pair into stable cluster geometry. The likelihood of a second AN molecule to be deposited near the cluster is statistically small enough to be ignored. As a consequence of the Franck−Condon principle, electronic excitation of the cluster forms the excited state in a strained matrix structure with respect to the most stable configuration of the excited state provided the geometry change is large (cf. Figures 11 and 12). Relaxed CT emission can therefore be observed in an argon matrix only if the geometrical change required for stabilizing the CT state (primarily motion of the AN ligand with respect to the pyrrole derivative) is small enough to be "permitted" by the matrix. A comparison between the trapping sites of the GS with those of the CT-state clusters leads to the following conclusions: (1) In the case of PBN, reorientation of the AN molecule to reach the optimal geometry of either of the CT minima is not likely to be possible in the matrix due to the large structural changes needed. Therefore emission must ensue from the "nascent" excited-state structure and addition of AN to argon has nearly no effect on the recorded emission spectrum.[10] (2) In the case of PP, the structure of the PP:AN 1:1 cluster in the ground state and the CT state are similar (Figures 2 and 8) so that relaxation of the cluster structure to reach the optimal geometry of the AQ form is restricted to a much lesser extent by the matrix. Nonetheless, the CT emission band recorded in the AN-doped matrix is much narrower than the one observed in AN solution (see Figure 6 of ref 9). This narrowing is probably an indication that the relaxation process is hindered and is a manifestation of the "matrix wall" effect.[10]

The small dependence on the excitation wavelength of the PBN emission spectrum in AN-doped argon matrixes is in sharp contrast to the strong dependence in the case of PP. Usually, strong wavelength dependence in rigid environment indicates an inhomogeneous distribution of sites.[42,43] Therefore, these experimental observations may indicate a rather narrow distribution of sites for PBN with AN (around the most stable PBN:AN isomer) compared to a broad distribution of sites for PP with AN. This is supported by the fact that the binding energy between PBN and AN is higher than between PP and PBN.

In argon matrixes doped by higher AN concentrations such as 4.7%,[10] sites in which each PBN molecule has two or three neighbors are likely to be formed. In this case, the second AN may be accidentally in the position to which the AN would have to move after CT excitation or the increased free volume may allow better alignment of AN with respect to PBN through relaxation. This explains the weak additional band, appearing as a shoulder at about 410 nm, observed at the higher concentration of AN in argon.

Photophysics of Phenylpyrrole Derivatives

*J. Phys. Chem. A, Vol. 109, No. 17, 2005* **3841**

*(3) Assignment of the CT-State Emission.* In neat argon the stabilization of the CT states is relatively small compared to the gas phase. The lowest lying CT state is therefore expected to be the Q from, which in the gas phase is lower than the AQ form. This explains the absence of CT emission in the case of neat argon matrixes containing PP, and its presence in the case of PBN (section IV(C)(2)): The small dipole moment of the Q form of PP is not sufficient to stabilize the CT state below the LE one, whereas the high dipole moment of PBN (around 11 D[13] for the Q state), stabilizes it in argon so it becomes the lowest excited state at its minimum energy.

In AN-doped argon matrixes the conditions change. The presence of AN as a nearest neighbor, in addition to the matrix effect, stabilizes the more polar AQ form ($\mu_{PP} \sim 10$ D, $\mu_{PBN} \sim 16$ D) so that it can become the lower CT state provided relaxation is possible. The emission from PP is probably from a hindered AQ form (with torsion angle between 40 and 90°)—the QC calculation shows that even planar antiquinoid PP has a large dipole moment.[13] The LE emission observed in AN-doped argon matrixes containing PP may be due to trapping sites in which no AN molecule is a nearest neighbor or those in which the location of the AN molecule is not favorable for CT stabilization.

The CT band observed from PBN in AN-doped matrixes is also likely to arise from a hindered AQ form (thus appearing at significantly higher energy[10] than in AN solution). But a contribution from the highly polar Q form cannot be ignored. The small shift with respect to the emission spectrum in neat argon is again explained by the matrix wall effect: the AN molecule cannot move inside the matrix so as to optimally stabilize the system (see Figure 9 of ref 10).

**(D) Implications for Liquid Solution of PP and PBN.** The solution phase can be considered as an intermediate between the gas phase (free motion) and the matrix (rigid medium) with respect to the freedom of relative motion between two bodies. The dynamics in solution are affected by the "cage effect", but the important factor is whether the system can relax to its equilibrium configuration during the lifetime of the excited state. This is often possible in liquid solutions in contrast with the case of a solid matrix, where large-amplitude motion is practically forbidden.

In the preceding section, it was surmised that the CT emission recorded from PBN in argon is likely to arise from both the quinoidal and antiquinoidal forms. A pertinent question is which form is the emitting CT species in liquid solution. Two factors have to be considered when passing from the matrix medium to the solution: First, the nearly free motion of the molecules in solution (allowing intramolecular and intermolecular relaxation) and the ability of the solvent medium to stabilize the CT state (which depends on the dielectric constant of the solvent and the dipole moment of the CT structure). Since two minima are found on the CT PES, the relative energy of these two CT forms has to be considered. In a medium with a low dielectric constant, the Q form will probably be lower than the AQ one (as in the isolated molecule). As the dielectric constant of the medium increases, the highly polar AQ form is expected to be lowered to a larger extent than the Q one, so that, in a solvent such as acetonitrile, the AQ form may be the emitting one. In molecules such as PP, in which the Q form has a very small dipole moment, CT fluorescence can be only from the AQ minimum. Finally, the results of this analysis suggest that in polar solvents direct optical excitation of the CT states should also be considered in the analysis of the absorption spectrum.

## V. Summary and Conclusions

In this paper a theoretical analysis of photophysical experiments on two molecules that emit dual fluorescence is presented. The emphasis is on low-temperature data obtained in supersonic jets and in cryogenic matrixes. The structures of 1:1 clusters of *N*-phenylpyrrole (PP) and pyrrolobenzonitrile (PBN) with acetonitrile (AN) are calculated using a variety of methods and used in simulations of the co-deposition of the pyrrolo derivatives and AN in an argon matrix.

In the argon matrix, the absence of CT emission from PP and its presence in the case of PBN are explained by the structures of the trapping sites and the higher dipole moment of the CT state of PBN. The data indicate that, in the cavity, the CT emitting species is either the Q form of PBN or a strained AQ form that is not free to attain the ultimate minimum due to the cage effect. Addition of AN does not lead to a notable change in the CT spectrum of PBN; this is consistent with the restricted possible motion of AN relative to PBN in the matrix. In the case of PP, a new CT emission band appeared (upon addition of AN) since the motion of AN required a minor perturbation of the matrix.

In addition, the structures of clusters of PP (or PBN) with several molecules of AN were obtained by a molecular mechanics simulation and used to explain the absence of CT emission from small clusters of PBN with acetonitrile, and its appearance in larger ones. The observation of only a single emission band in large clusters of PP with AN may be due to unresolved emissions from both LE and CT states, a point that requires further experimental elucidation.

**Supporting Information Available:** Atomic charges used for the MM calculation (Figure S1), structures of representative high-energy isomers of GS−PP:AN$_2$ and GS−PBN:AN$_2$ (Figure S2), of the most stable GS-PP:AN$_3$ and GS−PBN:AN$_3$ isomers (Figures S3 and S4), and of the lowest AQ−PP:AN$_n$ and AQ−PBN:AN$_n$ isomers, for $n = 2-4$ (Figure S5), and the trapping site of the isolated AN molecule (Figure S6). This material is available free of charge via the Internet at http://pubs.acs.org.

## References and Notes

(1) Grabowski, Z. R.; Rotkiewicz, K.; Rettig, W. *Chem. Rev.* **2003**, *103*, 3899.

(2) Zachariasse, K. A.; Grobys, M.; von der Haar, Th.; Hebecker, A.; Il'ichev, Yu. V.; Jiang, Y. B.; Morawski, O.; Kuhnle, W. *J. Photochem. Photobiol., A* **1996**, *102*, 59.

(3) Belau, L.; Haas, Y. *Chem. Phys. Lett.* **2002**, *364*, 157.

(4) Belau, L.; Haas, Y.; Rettig, W. *J. Phys. Chem. A* **2004**, *108*, 3916.

(5) Rettig, W.; Marschner, F. *Nouv. J. Chim.* **1983**, *7*, 425.

(6) Cornelissen-Gude, C.; Rettig, W. *J. Phys. Chem. A* **1998**, *102*, 7754.

(7) Sarkar, A.; Chakravorti, S. *Chem. Phys. Lett.* **1995**, *235*, 195.

(8) Yoshihara, T.; Galiewsky, V. A.; Druzhinin, I. S.; Saha, S.; Zachariasse, K. A. *Photochem. Photobiol. Sci.* **2003**, *2*, 342.

(9) Schweke, D.; Haas, Y. *J. Phys. Chem. A* **2003**, *107*, 9554.

(10) Schweke, D.; Baumgarten, H.; Haas, Y.; Rettig, W.; Dick, B. *J. Phys. Chem. A* **2005**, *109*, 576.

(11) Okuyama, K.; Numata, Y.; Odawara, S.; Suzuka, I. *J. Chem. Phys.* **1998**, *109*, 7185.

(12) Rotkiewicz, K.; Grellman, K. H.; Grabowski, Z. R. *Chem. Phys. Lett.* **1973**, *19*, 315.

(13) Zilberg, S.; Haas, Y. *J. Phys. Chem. A* **2002**, *106*, 1.

(14) Frisch, M. A.; Cheeseman, J. R.; Zakrzewski, V. G.; Montgomery, J. A., Jr.; Stratmann, R. E.; Burant, J. C.; Dapprich, S.; Millam, J. M.;

Daniels, A. D.; Kudin, K. N.; Strain, M. C.; Farkas, O.; Tomasi, J.; Barone, V.; Cossi, M.; Cammi, R.; Mennucci, B.; Pomelli, C.; Adamo, C.; Clifford, S.; Ochterski, J.; Petersson, G. A.; Ayala, P. Y.; Cui, Q.; Morokuma, K.; Malick, D. K.; Rabuck, A. D.; Raghavachari, K.; Foresman, J. B.; Cioslowski, J.; Ortiz, J. V.; Stefanov, B. B.; Liu, G.; Liashenko, A.; Piskorz, P.; Komaromi, I.; Gomperts, R.; Martin, R. L.; Fox, D. J.; Keith, T.; Al-Laham, M.; Wong, C. Y.; Peng, A.; Nanayakkara, C.; Gonzalez, M.; Challacombe, P. M. W.; Gill, B. G.; Johnson, W.; Chen, M. W.; Andres, J. L.; Head-Gordon, M.; Replogle, E. S.; Pople, J. A. *Gaussian 98*, revision A.9; Gaussian, Inc.: Pittsburgh, PA, 1998.

(15) Becke, A. D. *J. Chem. Phys.* **1934**, *98*, 5648.

(16) Lee, C.; Yang, W.; Parr, R. G. *Phys. Rev. B* **1988**, *37*, 785.

(17) Moller, C.; Plesset, M. S. *Phys. Rev.* **1934**, *46*, 618.

(18) Boys, S. F.; Bernardi, F. *Mol. Phys.* **1970**, *19*, 553.

(19) McDonald, N. A.; Jorgensen, W. L. *J. Phys. Chem. B* **1998**, *102*, 8049.

(20) Jorgensen, W. L.; Laird, E. R.; Nguyen, T. B.; Tirado-Rives, J. *J. Comput. Chem.* **1993**, *14*, 206.

(21) Bohm, H. J.; McDonald, I. R.; Maden, P. A. *Mol. Phys.* **1983**, *49*, 347.

(22) Singh, U. C.; Kollman, P. A. *J. Comput. Chem.* **1984**, *5*, 129.

(23) Powell, M. J. D. *Comput. J.* **1964**, *7*, 155.

(24) Powell, M. J. D. *Lecture Notes in Mathematics*; Springer: New York, 1984; Vol. 1066, pp 122−141. See also http://math.fullerton.edu/mathews/n2003/ PowellMethodMod.html.

(25) Old Powell: Press, W. H.; Teukolsky, S. A.; Vetterling, W. T.; Flannery, B. P. *Numerical Recipes in FORTRAN, the Art of Scientific Computing*; Cambridge University Press: Cambridge, U.K., 1992; p 387 ff. New Powell: Powell, M. J. D. "Optimization Methods and Software",

Program NEWUOA; Report No. DAMTP 2003/NA03, University of Cambridge: Cambridge, U.K., 2003.

(26) Fraenkel, R.; Haas, Y. *Chem. Phys.* **1994**, *186*, 185.

(27) Fraenkel, R.; Schweke, D.; Haas, Y.; Molnar, F.; Horinek, D.; Dick, B. *J. Phys. Chem. A* **2000**, *104*, 3786.

(28) Klein, M. L.; Venables, J. A. *Rare Gas Solids*; Academic Press: New York, 1976.

(29) Andersen, H. C. *J.* Comput. Phys. **1983**, *52*, 24.

(30) Siebers, J. G.; Buck, U.; Beu, T. A. *Chem. Phys.* **1998**, *239*, 549.

(31) El-Shall, M. S.; Daly, G. M.; Wright, D. *J. Chem. Phys.* **2002**, *116*, 23.

(32) Sun, S.; Bernstein, E. R. *J. Phys. Chem.* **1996**, *100*, 1334.

(33) Barrow, M. J. *Acta Crystallogr.* **1981**, *B37*, 2239.

(34) Crepin, C.; de Pujo, P.; Bouvier, B.; Brenner, V.; Millie, Ph. *Chem. Phys.* **2001**, *272*, 243.

(35) George, L.; Shanchez-Gracia, E.; Sander, W. *J. Phys. Chem. A* **2003**, *107*, 6850.

(36) Chalasinski, G.; Szczesniak, M. M. *Chem. Rev.* **2000**, *100*, 11.

(37) Gotch, A. J.; Zwier, T. S. *J. Chem. Phys.* **1991**, *96*, 3388.

(38) Garrett, A. W.; Severance, D. L.; Zwier, T. S. *J. Chem. Phys.* **1991**, *95*, 9699.

(39) Gord, J. R.; Garrett, A. W.; Bandy, R. E.; Zwier, T. S. *Chem. Phys. Lett.* **1990**, *171*, 44.

(40) Hineman, M. F.; Kim, S. K.; Bernstein, E. R.; Kelley, D. F. *J. Chem. Phys.* **1992**, *96*, 4904.

(41) Nimlos, N. R.; Young, M. A.; Bernstein, E. R.; Kelley, D. F. *J. Chem. Phys.* **1989**, *91*, 5268.

(42) Haas, Y.; Samuni, U. *Prog. React.* Kinet. **1998**, *23*, 211.

(43) Al-Hassan, K. A.; Rettig, W. *Chem. Phys. Lett.* **1986**, *126*, 273.